Water Splitting

DOI: 10.1002/anie.201203560

Surface-Immobilized Single-Site Iridium Complexes for Electrocatalytic Water Splitting**

Khurram Saleem Joya, Navaneetha K. Subbaiyan, Francis D'Souza, and Huub J. M. de Groot**

Catalytic water splitting using solar energy represents an attractive potential solution for affordable and renewable energy.[1,2] To construct a (photo)electrochemical H_2/O_2 evolution system, oxygen evolving catalysts (OECs) need to be immobilized on a conducting surface.[1] Many metal complexes containing single or more catalytic sites have been tested for water oxidation;[2–7] however, the design and implementation of a stable and efficient molecular water oxidation system that operates at high catalytic turnover number (TON) and frequency (TOF) for extended periods of controlled-potential electrolysis (CPE), with moderate overpotential and high current density, are challenging.[8–10]

Herein we disclose robust immobilized $[(L_2bpy)Ir^{III}Cp^*(OH_2)]^{2+}$ (L is $-PO_3H_2$ or -COOH, bpy is 2,2′-bipyridine, Cp* is pentamethylcyclopentadiene) complexes on ITO (indium tin oxide) surface (ITO/Cat) for electrocatalytic water oxidation (Figure 1). The aqua complexes were obtained by Cl to H_2O ligand exchange before immobilization on the ITO surfaces. The mono-iridium catalysts are modified with carboxylate and phosphonate linkers that are known to anchor covalently on ITO.[1,9] At 1.75 V (vs. NHE; NHE = normal hydrogen electrode) the system operates with a high TOF of 6.7 s^{-1} and has TONs of more than 210000, well in excess of the maximum TON of 28000 reported before.[9] The oxygen generation current densities are higher than 1.70 mA cm^{-2}, which is one to two orders of magnitude higher than the reported densities of approximately 50 μA cm^{-2}.[8,9] Without linker units the complex $[(bpy)Ir^{III}Cp^*(OH_2)]^{2+}$ (Cat.**Ir**-bpy) is active for homogeneous water oxidation. Electrochemical quartz crystal nanobalance (EQCN) experiments[11] show no sign of metal oxide deposition during catalytic cycling. Cyclic voltammetry (CV) analysis, CPE, EQCN, and homogeneous catalysis data provide converging evidence that the surface-anchored $[(L_2bpy)Ir^{III}Cp^*(OH_2)]^{2+}$ molecular complex is a highly competent catalytic system for electrochemical oxygen evolution.

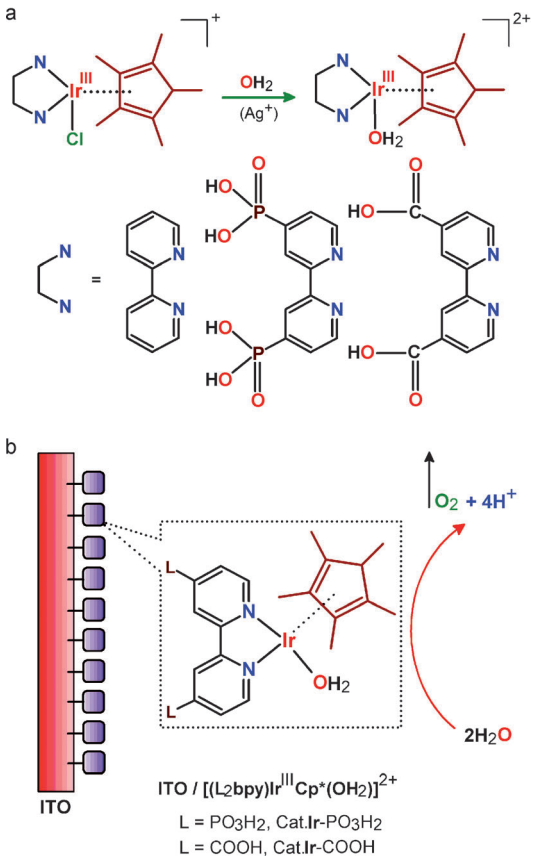

Figure 1. a) Cp*–Ir-derived complexes with bpy and L_2bpy ligands; b) Schematic representation of the immobilized $[(L_2bpy)Ir^{III}Cp^*(OH_2)]^{2+}$ (Cat.**Ir**-PO_3H_2 and Cat.**Ir**-COOH for L = PO_3H_2 and COOH, respectively) on ITO for electrochemical water oxidation. The metal-stabilizing Cp* ligand is highlighted in brown-red.

The synthesis and characterization of the complexes are detailed in the Supporting Information (Figure S1).[12,13] In situ ligand exchange from Cl to H_2O and deprotonation are monitored by UV/Vis spectroscopy (Figure S2 in the Supporting Information). CV of an ITO/Cat.**Ir**-COOH in aqueous acid (pH 1) shows a catalytic current wave at approximately 1.22 V that sharply grows until approximately 1.31 V, and leads to an O_2 evolution current with tiny oxygen

[*] Dr. K. S. Joya, Prof. H. J. M. de Groot
Leiden Institute of Chemistry, Leiden University
Einsteinweg 55, P.O. Box 9502, 2300 RA, Leiden (The Netherlands)
E-mail: khurramsj@chem.leidenuniv.nl
ssnmr@chem.leidenuniv.nl
Dr. K. S. Joya
Department of Chemistry
University of Engineering and Technology (UET)
GT Road, 54890, Lahore, Punjab (Pakistan)
Dr. N. K. Subbaiyan, Prof. F. D'Souza
Department of Chemistry, University of North Texas
1155 Union Circle, #305070, Denton, TX 76203 (USA)

[**] K.S.J. acknowledges the Higher Education Commission (HEC), Pakistan, for the research grant. We also thank Dr. Yasir Faheem for help in electrode surface preparation. This work is also partially supported by National Science Foundation (Grant No. 1110942 to F.D.) and by the BioSolar Cells open innovation program of the Netherlands Ministry of Economic Affairs, Agriculture and Innovation.

Supporting information (including experimental procedures) for this article is available on the WWW under http://dx.doi.org/10.1002/anie.201203560.

bubbles visible above 1.51 V (vs. NHE). During the reverse scan a broader reduction wave is observed until 1.20 V (Figure 2). In neutral buffer solution (pH 7), a polarization wave appears at approximately 0.91 V and rapidly raises at approximately 1.11 V. The forward sweep current wave can be assigned to two simultaneous proton-coupled electron transfer (PCET) events, $\{Ir^{IV}(OH)\}^{2+}/\{Ir^{III}(OH_2)\}^{2+}$ and $\{Ir^{V}(=O)\}^{2+}/\{Ir^{IV}(OH)\}^{2+}$ (Scheme 1).[14]

Alternatively, two oxidations of the iridium center in $\{Ir^{III}(OH_2)\}^{2+}$ can also occur at almost the same potential; in this case $\{Ir^{IV}(OH)\}^{2+}$ is a "missing" oxidation state, as it was not detected (Scheme 1 (I)).[14,15] At pH 7 the oxygen onset potential remains above 1.51 V. This value contrasts with the shift of approximately 60 mV/pH unit for the oxygen onset potential; this shift is considered an essential characteristic of the iridium oxide based catalytic system and thus the observed value shows that the rate-determining electron transfer step is not coupled to proton transfer.[1,13,16] The complexes are stable on the anode, and repeating the CV reproduces the voltammogram well for the ITO/Cat.**Ir**-COOH assembly (Figure S3 in the Supporting Information. The ITO/Cat systems after CV measurements were employed for long-term CPE of water. Current densities $J > 1.70\ mA\,cm^{-2}$ can be sustained for many hours with little degradation over time for ITO/Cat.**Ir**-COOH and ITO/Cat.**Ir**-PO_3H_2 during electrocatalysis at 1.75 V (vs. NHE); in contrast current densities below $25\ \mu A\,cm^{-2}$ were observed in the blank ITO run (Figure 3). O_2 bubbles were leaving the ITO/Cat surface along with simultaneous H_2 generation at the spiral Pt electrode in the cathodic compartment.

The CPE initiates at high initial current densities, $J > 1.85\ mA\,cm^{-2}$, with O_2 formation starting within seconds of the electrolysis operation (Figure S4 in the Supporting Information). Increase in the current densities for O_2 evolution during CPE owing to a time-dependent build-up of catalytic deposits on the surface was not observed (Figure 3). Cyclic voltammograms obtained for ITO/Cat.**Ir**-PO_3H_2 at various intervals during CPE remain unchanged and indicate the robustness of the surface-anchored molecular assembly (Figure S5 in the Supporting Information). The ITO/Cat.**Ir**-PO_3H_2 complex generates more than 400 μmol of O_2 in 13 h of CPE; this rate corresponds to a TON higher than 2.1×10^5 (Figure 4). The ITO/Cat.**Ir**-PO_3H_2 makes O_2 at a rate of approximately $6.8\ mol\,s^{-1}$ per mole of catalyst. The ITO/Cat.**Ir**-COOH produces more than 340 μmol of oxygen during 11 h of electrolysis operation at a TOF of higher than 6.7 moles of O_2 per second per mole of catalyst (inset Figure 4). Thus, the surface-anchored Cat.**Ir**-PO_3H_2 and Cat.**Ir**-COOH catalysts exhibit strongly enhanced catalytic performance compared to other catalysts, such as an anodically tested triaqua Cp*–Ir complex (pH 6) and CoO_x–phosphate (pH 7) with only TON ≤ 10 at rates of $1.46\ s^{-1}$ and $0.05\ s^{-1}$, respectively.[9b,10]

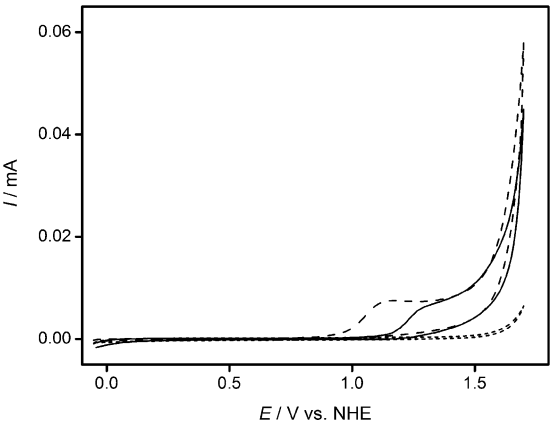

Figure 2. Cyclic voltammograms for the blank ITO (-----) and ITO/Cat.**Ir**-COOH in deoxygenated aqueous HNO_3 (0.1 M, pH 1; ——) and phosphate buffer (0.1 M, pH 7; – – –). Scan rate: $50\ mV\,s^{-1}$; ITO area $A = 0.5\ cm^2$.

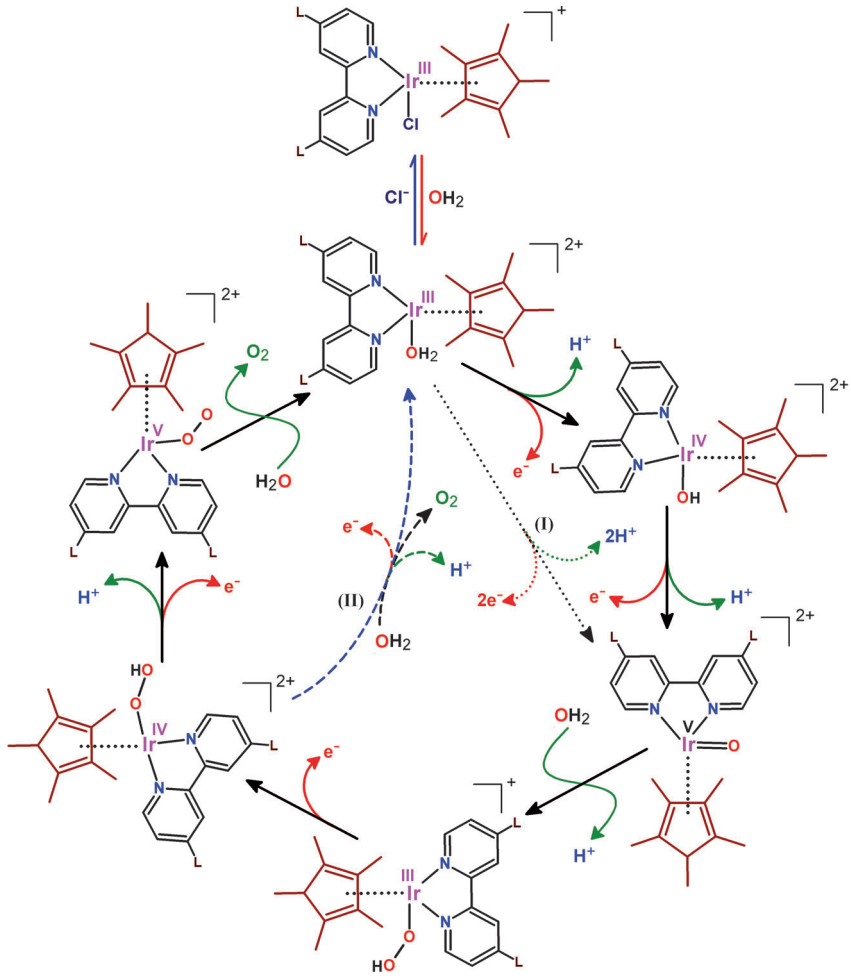

Scheme 1. Proposed water oxidation mechanism and O–O bond formation by the $[(L_2bpy)Ir^{III}Cp^*(OH_2)]^{2+}$ complex.

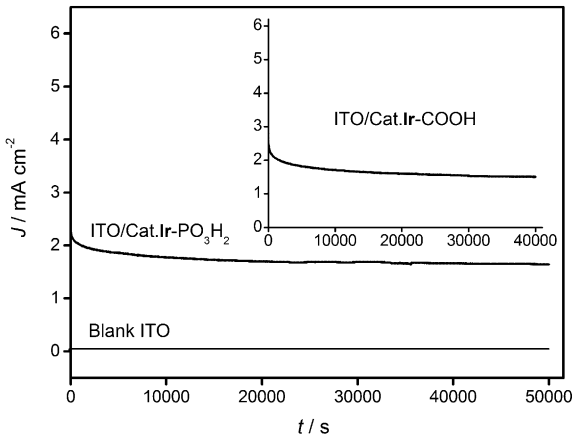

Figure 3. Controlled-potential water electrolysis with the ITO, ITO/Cat.**Ir**-PO_3H_2, and ITO/Cat.**Ir**-COOH (inset) in deoxygenated buffer solution (0.1 M, pH 4) at 1.75 V (vs. NHE). Catalyst density = 1.55–1.75×10^{-10} mol cm^{-2}.

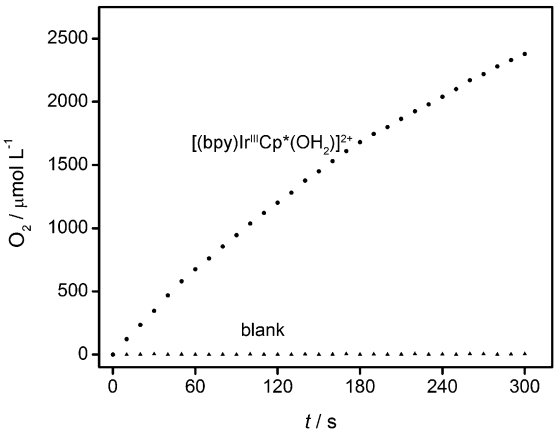

Figure 5. Oxygen evolution (initial rate) during homogeneous water oxidation by the $[(bpy)Ir^{III}Cp^*(OH_2)]^{2+}$ catalyst in aqueous deoxygenated HNO_3 (0.1 M) with Ce^{IV} (50 mM). Catalyst concentration (25.0 ± 0.2) μmol L^{-1}.

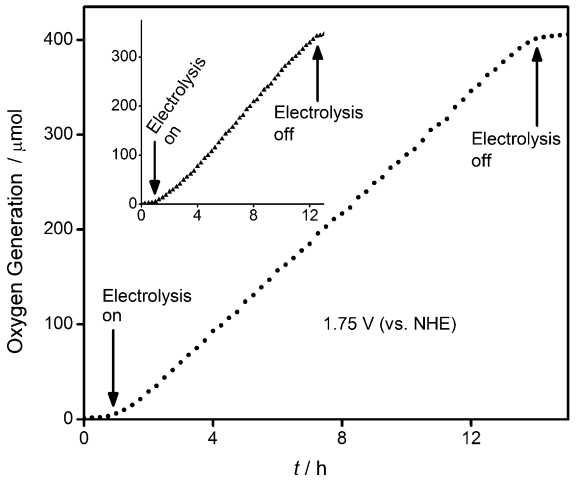

Figure 4. O_2 generation for water electro-oxidation with ITO/Cat.**Ir**-PO_3H_2 and ITO/Cat.**Ir**-COOH (inset) in buffer solution (0.1 M, pH 4).

In homogeneous catalysis experiments, the corresponding aqua iridium complex Cat.**Ir**-bpy shows a higher initial rate for oxygen evolution than the halogen analogues.[15] Furthermore, with the aqua complexes that were obtained after Cl to H_2O ligand exchange, the catalysis initiates within seconds of the Ce^{IV} addition, and the initial lag time observed in the homogeneous water oxidation catalysis by the halogen-bonded analogues is avoided (Figure 5).[15b] The rate of oxygen evolution attains its maximum value within 1–2 min, and afterwards the rate starts to decrease slowly (Figure 5). For prolonged catalysis during five hours, $[(bpy)Ir^{III}Cp^*(OH_2)]^{2+}$ shows a TON of 1500. This number is much higher than for the chloro and iodo analogues and confirms the increased durability obtained by exchanging the halogen group to the H_2O ligand before the catalysis (Table S1 in the Supporting Information). The initial rate of O_2 evolution for Cat.**Ir**-bpy is 27 min^{-1}, which is also higher than for the mono-iridium chloro complexes.[6,15]

To confirm the molecular integrity of our surface-anchored complexes and to probe if there is any electrodeposition or metal oxide formation, we performed high-sensitivity in situ EQCN studies.[11,17] The experiments are undertaken while scanning the potential between 0 and 1.6 V (vs. NHE), and during this scan O_2 evolution occurs. The effect of mass (ng) changes on the gold-coated piezoelectric quartz (Au-PZT), which was used as the working electrode, is monitored by recording frequency changes. The EQCN experiments for a blank solution during four potential cycles reveals no mass gain on the Au-PZT disk (Figure 6). Only small and reversible variations are detected during the forward scan owing to some oxygen evolution and reorganization of the gold surface that is relieved in the reverse sweep.[17] The result for an EQCN study with Ir catalysts for four potential cycles is shown in Figure 6. The EQCN response with Ir catalysts looks very similar to the background experiment and there is no indication of mass gain in the potential window for water oxidation. Each CV cycle reproduces essentially the same mass response, thus effectively eliminating the possibility that the formation of surface species by electrodeposition, such as iridium oxide, is required to initiate water oxidation (Figure S6 in the Supporting Information).[11,17] This finding corroborates and confirms the experimental evidence obtained from the CV, CPE, and homogeneous catalysis data that the ITO/Cat.**Ir**-COOH and ITO/Cat.**Ir**-PO_3H_2 remain intact and are the active species during the surface electrocatalysis.

It was recently reported for $[Cp^*Ir^{III}(N{-}C)(OH_2)]^+$ and $[Cp^*Ir^{III}(N{-}N)(OH_2)]^{2+}$ complexes that iridium–oxo species $\{Ir^V(=O)\}^{n+}$ ($n=1$ for N–C and 2 for N–N) are generated from $\{Ir^{III}(OH_2)\}^{n+}$ oxidation with simultaneous removal of two protons.[15] The O–O bond formation possibly proceeds by the nucleophilic attack of a OH_2 molecule to an $\{Ir^V(=O)\}^{n+}$ intermediate (Scheme 1). At the same time, a proton is thought to leave from the arriving water molecule to form a hydroxide ion that enhances the nucleophilicity for the attack at the iridium–oxo complex.[15b] The cyclic voltam-

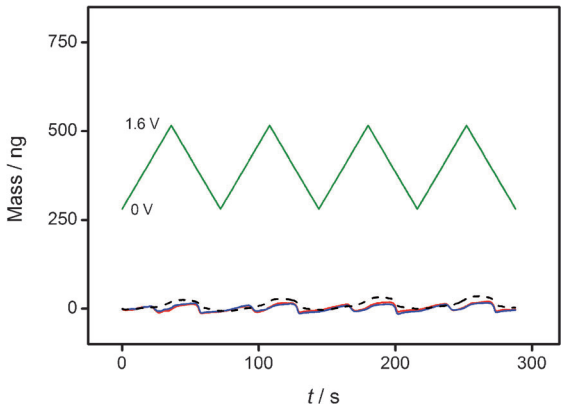

Figure 6. EQCN mass response as a function of time during four consecutive CV cycles (0–1.6 V vs. NHE; indicated by the green line) for Cat.**Ir**-PO_3H_2 (blue line) and Cat.**Ir**-COOH (red line) in deoxygenated HNO_3 (0.1 M) solution. The dashed line corresponds to the background signal. The concentrations of Ir catalysts were 2 mg/15 mL solution.

mograms presented in Figure 2 point to a mechanism where, after the second OH_2 insertion, the next electron removal is not coupled with the proton transfer, because the O_2 onset potential is not in agreement with the pH dependence of 60 mV/pH unit according to the Nernst law.[16] To uncouple the electron and proton transfer, most likely the $\{Ir^{III}(-OOH)\}^{(n-1)+}$ complex is formed by deprotonation accompanying the second OH_2 ligation to the $\{Ir^{V}(=O)\}^{n+}$. This species can release an electron to form an $\{Ir^{IV}(-OOH)\}^{n+}$-type intermediate in the next step (Scheme 1), then loses the fourth electron and proton, and generates dioxygen while recoordinating to another OH_2 to regenerate the aqua complex for the next catalytic turnover.[15]

Since the catalyst shows a fast rate for oxygen evolution, the last OH_2 ligation is not likely to be the rate-limiting step and the $\{Ir^{V}(-OO)\}^{n+}$ may not be a reaction intermediate but a lowered transition state or transient species (Scheme 1 (II)). Most probably the large bite angle between the bpy-Ir and Cp* moieties provides a wide gap to facilitate rapid OH_2 insertion at the beginning of the second half of the water oxidation cycle. Moreover, the strong electron-donating character of the Cp* ligand helps to stabilize the complex and intermediates during the catalytic cycle.[13,15] Studies are performed to gain further insight into how the catalysis is integrated with transient storage of charge to produce an enhanced surface catalytic process of four electron removal and associated proton release during the water oxidation cycle and O–O bond formation.[13]

In conclusion, we presented herein efficient and easily accessible mono-iridium complexes that are catalytically very active and robust when tethered to an ITO surface. Water oxidation was realized just above 1.51 V (vs. NHE) on ITO/Cat assemblies, and TONs higher than 2.1×10^5 per catalyst molecule were obtained during prolonged periods of CPE. Under steady-state conditions, the ITO/Cat assemblies show a TOF above 6.7 s^{-1} with a current density of approximately 1.70 mA cm^{-2} and generate more than 400 μmol of O_2. Reproducible cyclic voltammograms obtained in solutions at pH 1 and pH 7 reveal invariance of the oxygen onset potential upon increase of the pH and exclude the involvement of a catalytic species that operates with four PCET steps exhibiting a shift of approximately 60 mV/pH unit, as is observed for iridium oxides.[1,16] In parallel, a high initial current density and rapid onset of oxygen evolution in CPE provide additional evidence for the involvement of activated molecular aquo species on the ITO anode in catalyzing the water oxidation. The rapid onset of catalytic activity of the molecular system was validated in homogeneous water oxidation assays. Finally, to strengthen our claim for the molecular integrity of the $[(L_2bpy)Ir^{III}Cp^*(OH_2)]^{2+}$ catalysts during electrochemical oxygen generation, we performed in situ EQCN experiments and verified that there is no net mass increase during potential cycling. This result leads us to conclude that the present mono-iridium complexes represent a highly competent molecular system for water oxidation. We anticipate that this study will help to pave the way for photoelectrocatalytic devices with immobilized mono-site molecular complexes for future fuel generation from water splitting.

Received: May 8, 2012
Published online: August 22, 2012

Keywords: catalysis · electrochemistry · iridium · solar energy · water splitting

[1] K. S. Joya, H. J. M. de Groot, *Int. J. Hydrogen Energy* **2012**, *37*, 8787 – 8799.
[2] J. Limburg, J. S. Vrettos, L. M. Liable-Sands, A. L. Rheingold, R. H. Crabtree, G. W. Brudvig, *Science* **1999**, *283*, 1524 – 1527.
[3] R. Lalrempuia, N. D. McDaniel, H. Müller-Bunz, S. Bernhard, M. Albrecht, *Angew. Chem.* **2010**, *122*, 9959 – 9962; *Angew. Chem. Int. Ed.* **2010**, *49*, 9765 – 9768.
[4] P. Kurz, G. Berggren, M. F. Anderlund, S. Styring, *Dalton Trans.* **2007**, 4258 – 4261.
[5] L. Tong, L. Duan, Y. Xu, T. Privalov, L. Sun, *Angew. Chem.* **2011**, *123*, 465 – 469; *Angew. Chem. Int. Ed.* **2011**, *50*, 445 – 449.
[6] A. Savini, G. Bellachioma, G. Ciancaleoni, C. Zuccaccia, D. Zuccaccia, A. Macchioni, *Chem. Commun.* **2010**, *46*, 9218 – 9219.
[7] D. J. Wasylenko, C. Ganesamoorthy, M. A. Henderson, B. D. Koivisto, H. D. Osthoff, C. P. Berlinguette, *J. Am. Chem. Soc.* **2010**, *132*, 16094 – 16106.
[8] T. Wada, K. Tsuge, K. Tanaka, *Angew. Chem.* **2000**, *112*, 1539 – 1542; *Angew. Chem. Int. Ed.* **2000**, *39*, 1479 – 1482.
[9] a) J. J. Concepcion, J. W. Jurss, P. G. Hoertz, T. J. Meyer, *Angew. Chem.* **2009**, *121*, 9637 – 9640; *Angew. Chem. Int. Ed.* **2009**, *48*, 9473 – 9476; b) X. Sala, I. Romero, M. Rodríguez, L. Escriche, A. Llobet, *Angew. Chem.* **2009**, *121*, 2882 – 2893; *Angew. Chem. Int. Ed.* **2009**, *48*, 2842 – 2852.
[10] J. D. Blakemore, N. D. Schley, G. W. Olack, C. D. Incarvito, G. W. Brudvig, R. H. Crabtree, *Chem. Sci.* **2011**, *2*, 94 – 98.
[11] T. J. Meyer, *Nat. Chem.* **2011**, *3*, 757 – 758.
[12] a) K. S. Joya, H. J. M. de Groot, Netherlands Patent Application no. 2005512; Oct **2010**, Granted as: WIPO Patent Application WO/2012/050436 (April 19, **2012**; b) International Patent Application no. PCT/NL2011/050673; Oct **2011**.
[13] J. L. Vallés-Pardo, M. C. Guijt, M. Iannuzzi, K. S. Joya, H. J. M. de Groot, F. Buda, *ChemPhysChem* **2012**, *13*, 140 – 146.

[14] J. J. Concepcion, J. W. Jurss, J. L. Templeton, T. J. Meyer, *J. Am. Chem. Soc.* **2008**, *130*, 16462 – 16463.
[15] a) J. F. Hull, D. Balcells, J. D. Blakemore, C. D. Incarvito, O. Eisenstein, G. W. Brudvig, R. H. Crabtree, *J. Am. Chem. Soc.* **2009**, *131*, 8730 – 8731; b) J. D. Blakemore, N. D. Schley, D. Balcells, J. F. Hull, G. W. Olack, C. D. Incarvito, O. Eisenstein, G. W. Brudvig, R. H. Crabtree, *J. Am. Chem. Soc.* **2010**, *132*, 16017 – 16029.
[16] T. Nakagawa, C. A. Beasley, R. W. Murray, *J. Phys. Chem. C* **2009**, *113*, 12958 – 12961.
[17] N. D. Schley, J. D. Blakemore, N. K. Subbaiyan, C. D. Incarvito, F. D'Souza, R. H. Crabtree, G. W. Brudvig, *J. Am. Chem. Soc.* **2011**, *133*, 10473 – 10481.

